Revista Brasileira de Engenharia Biomédica,
v. 24, n. 2, p. 131-137, agosto 2008

ISSN 1517-3151
http://dx.doi.org/10.4322/rbeb.2012.055

Comunicação Técnica
Recebido em 30/07/2007, aceito em 25/08/2008

Spectral analysis of respiratory flow and gas concentrations

Análise espectral de fluxo e concentrações de gases respiratórios

Marcelo Alexandre Garcia
Laboratório de Engenharia Biomédica
Escola Politécnica / USP

Newton Nunes
Maria Urbana Pinto Brandão Rondon
Ana Maria Fonseca Wanderley Braga
Carlos Eduardo Negrão
Instituto do Coração, Faculdade de Medicina / USP

José Carlos Teixeira de Barros Moraes*
Laboratório de Engenharia Biomédica
Escola Politécnica / USP
Av. Prof. Luciano Gualberto, trav. 3, n. 158, sl. D2-05
05508-900 São Paulo, SP
E-mail: jcmoraes@leb.usp.br

*Corresponding author

Abstract
In this research we obtained samples of human respiratory flow, oxygen concentration and carbon dioxide concentration signals from 20 healthy subjects and evaluated the average power spectral density (PSD) of these signals. For each subject, the respiratory samples were acquired in four progressive levels of exercise in a cycle ergometer. Autoregressive moving average models were designed to represent the PSD found in each phase. An average PSD of the four levels was also calculated. Results have shown that the bandwidth of O_2 concentration, CO_2 concentration and flow signals was 8 Hz, 7 Hz, and 15 Hz, respectively, within the dynamic range of 50 dB. The PSD curves found can be used for optimal filter design for signal enhancing in fast on-line measurement of these signals.

Keywords: Respiratory signals, Spectral analysis, Dynamic response compensation, Breath-by-breath analysis.

Resumo
Nesta pesquisa foram registradas amostras dos sinais respiratórios de fluxo, concentração de oxigênio e concentração de gás carbônico em 20 voluntários saudáveis. A densidade espectral de potência (DEP) média foi então calculada. Para cada voluntário, as amostras dos sinais foram registradas em quatro intensidades progressivas de esforço físico em uma bicicleta ergométrica. Para representar a DEP encontrada em cada fase foram ajustados modelos auto-regressivos de média móvel. Uma DEP média entre as quatro intensidades também é fornecida. Os resultados mostraram que as larguras de banda dos sinais de concentração de O_2, concentração de CO_2 e fluxo foram 8 Hz, 7 Hz e 15 Hz, respectivamente, dentro de uma faixa dinâmica de 50 dB. As curvas de DEP encontradas podem ser usadas em projetos de filtros ótimos para equalização destes sinais em medições em tempo real.

Palavras-chave: *Sinais respiratórios, Análise espectral, Compensação de resposta dinâmica, Análise respiração-a-respiração.*

Introduction

Exercise stress testing has been widely employed to physical fitness assessment, cardiac disease diagnosis, cardiac rehabilitation and exercise prescription (White and Evans, 2001). The use of gas analysis with the stress testing, termed cardiopulmonary exercise testing, can be of particular value in distinguishing the cause of an individual's exercise limitation (Myers and Madhavan, 2001; Singh, 2001). The cardiopulmonary exercise test can be performed with the use of an ergospirometer, which is a clinical equipment that basically acquires, in real time, three signals from subject's airway: flow ($\dot{V}$), concentration of O_2 (FO_2), and concentration of CO_2 (FCO_2), while the load of an ergometer is controlled by a previously programmed protocol (ATS/ACCP, 2003; Madama, 1993). From these signals, the instrument can evaluate several parameters, such as oxygen uptake ($\dot{V}O_2$), carbon dioxide production ($\dot{V}CO_2$) and ventilation ($\dot{V}E$). The gas exchange in patient airways ($\dot{V}O_2$ and $\dot{V}CO_2$) originates from the energy metabolism (Ferrannini, 1988).

Previous studies (e.g. Farmery and Hahn, 2000; Noguchi *et al.*, 1982; Shykoff and Swanson, 1987) demonstrated that some compensation for the narrow dynamic range of mass spectrometers must be employed in order to improve the accuracy of gas exchange measurements. In the last decades mass spectrometers have been replaced by small transducer devices for ergospirometry purposes with similar signal passband, which suggests that dynamic response compensation must be applied to those transducers.

The spectral analysis of human $\dot{V}$, FO_2 and FCO_2 can be used to design Wiener filters (Kailath *et al.*, 2000) for optimal signal equalization for transducers of those signals. A Wiener filter minimizes the mean-square error (MSE) between the true signal and its measurement. It can be designed with knowledge of the power spectral density (PSD) of the true measured signal, the dynamic response of the transducer used to measure it and the PSD of the background noise of the transducer output signal. The transducer dynamic response is supposed to be linear and the background noise is supposed to be a random signal. Such filters for respiratory signal enhancement have been already mentioned by Bates *et al.* (1983) and Garcia *et al.* (2002). Garcia *et al.* (2002) designed a Wiener filter approximation by forcing a constant input signal power spectral density for the whole dynamic range.

Lemen *et al.* (1982) evaluated the PSD of $\dot{V}$ signal only for determination of the dynamic response required of devices to reproduce flow signal. However, the spectral analysis of respiratory signals in human beings during conditions of clinical ergospirometric stress tests have not been studied yet. Knowledge of the PSD of signals such as $\dot{V}$, FO_2 and FCO_2 is essential for optimal design of Wiener filters for those tests. Wiener filtering can give the lowest mean-square error possible between the true air flow or gas concentration and its measurement.

The objective of this work is to evaluate the average power spectral density of $\dot{V}$, FO_2 and FCO_2 signals from healthy subjects at four progressive levels of exercise in a cycle ergometer.

Methods

Subjects

This study was approved by the Human Research Ethics Committee of the Heart Institute (InCor) and the Clinics Hospital of the University of São Paulo. After giving their written consent, 20 healthy subjects (14 men and 6 women) performed the protocol described below. Their physical and functional characteristics are shown in Table 1.

Table 1. Physical and functional characteristics of the volunteers.

Age [years]	31 ± 6
Weight [kg]	75 ± 16
Height [cm]	174 ± 8
Maximal workload [W]	239 ± 63
$\dot{V}O_2$max. [ml/kg·min]	39 ± 10

Values are means ± SD; N = 20.

Protocol

Each subject performed a previous pulmonary stress exam in an ergospirometer MGC model Cad/Net System 2001. At this exam, the oxygen uptake ($\dot{V}O_2$) was evaluated at three reference points: ventilatory threshold ($\dot{V}O_2$vt) detected with the V-Slope technique (Beaver *et al.*, 1986); respiratory compensation point ($\dot{V}O_2$ rcp) (Beaver *et al.*, 1986); and peak oxygen uptake ($\dot{V}O_2$peak). A ramp protocol in a cycle ergometer with power increasing rate between 15 and 40 W/min was used, allowing each subject to complete the exam in an interval between 8 and 12 minutes.

The signal acquisition session was done at least 7 days after the previous exam. In this session, each subject worked on the cycle ergometer in four increasing power levels. In the beginning of each phase, the cycle ergometer power was set according to equation (1), as suggested by Lear *et al.* (1999):

$$\dot{V}O_2\,[ml/kg{\cdot}min] = Power\,[W] \cdot 12 + Bodyweight\,[kg] \cdot 3.5 \quad (1)$$

Equation (1) was used to choose the cycle ergometer power in order to reach the following oxygen uptake levels:

- Phase 1: 0-watt (rest): the subject remained stopped on the cycle ergometer in the same position in which the next phases were executed;
- Phase 2: power set to aim 25% of $\dot{V}O_2$ peak (volunteers achieved 22% ± 3% of $\dot{V}O_2$);
- Phase 3: power set to aim $\dot{V}O_2$vt (volunteers achieved 86% ± 11% of $\dot{V}O_2$vt);
- Phase 4: power set to aim 90% of $\dot{V}O_2$rcp (volunteers achieved 84 ± 6% of $\dot{V}O_2$rcp).

Each phase started with $\dot{V}O_2$ and $\dot{V}CO_2$ being measured with a Medgraphics Cad/Net System 2001. After the subject achieved steady values of $\dot{V}O_2$ and $\dot{V}CO_2$, which occurred typically 3 to 4 minutes after the beginning of the phase, O_2 and CO_2 concentrations and flow signals were registered for 1 minute. Then, the power was increased to the next phase. It was possible, with this protocol, to get 1-minute signal samples at four progressive levels of exercise for each subject.

Acquisition instruments

After reaching stationary rates in $\dot{V}O_2$ and $\dot{V}CO_2$, respiratory signals were acquired with a pneumotachometer (Medgraphics, model PreVent) coupled with a differential pressure transducer (Validyne, model MP45-14-871) and a carrier demodulator (Validyne, model CD19A). Gas concentrations were measured with a paramagnetic O_2 transducer (Servomex, model PM1111-E) with fast-response tubing configuration (rise time ($t_{10\text{-}90}$) and fall time ($t_{90\text{-}10}$) from 16 to 21% of O_2 are lesser than 200 ms) and an infrared CO_2 transducer (Servomex, model Ir1507). A sampling tube with a length of 2.4 m and an internal diameter of 1.15 mm and a flow controller (AEI Technologies, model R-1) set to 200 ml/min were used. Analog signals were registered with a 16-bit acquisition board (National Instruments, model PCI-6052E). Acquisition and signal processing were made with MATLAB® 6.0 package. Signals were acquired at a sampling rate of 100 Hz. The dynamic response of gas concentration transducers was compensated with equalizer filters based on the previous work described by Garcia *et al.* (2002). With this procedure, we extended the frequency range of the transducers to the range of 0 to 15 Hz. The Wiener filters guaranteed a flat gain response in this range.

Average PSD computation

The spectral analysis of each 1-minute sample was done with Welch's averaged modified periodogram method (Welch, 1967). Average power spectral densities were calculated for each phase individually, and for all 4 phases combined.

AR-MA model for signal power spectral density

Autoregressive moving average (AR-MA) models (Aström and Wittenmark, 1990; Ljung, 1999; Söderström and Stoica, 1989) were designed for each power spectral density (PSD) analysis, in order to obtain a parametric representation of these curves. The parametric models allowed us to represent each PSD curve shape with few parameters in the Results section. The structure of the model is shown in equation (2):

$$X(z) = \frac{C(z)}{A(z)} \cdot E(z) \quad (2)$$

where: $x(n)=Z^{-1}\{X(z)\}$ is the signal obtained at the output of the model with the same PSD of a true respiratory signal represented by the model; $e(n)=Z^{-1}\{E(z)\}$ is a normalized white noise signal; $C(z)$ and $A(z)$ are the polynomials of the AR-MA model (Proakis and Manolakis, 1996), as shown in equation (3).

$$\frac{C(z)}{A(z)} = k \cdot \frac{(z - zr_1)\cdot(z - zr_2)\cdot\cdots\cdot(z - zr_m)}{(z - pl_1)\cdot(z - pl_2)\cdot\cdots\cdot(z - pl_p)} \quad (3)$$

where: $z=e^{j\omega}$ is the complex frequency domain; m and p are the orders of polynomials $C(z)$ and $A(z)$, respectively; zr_i and pl_i are the zeroes and poles of the transfer function C/A, respectively; k is a constant gain.

The order of polynomials C and A were optimized based on the Akaike information criterion - AIC (Akaike, 1981). AR-MA model coefficients were obtained with the least squares method (Ljung, 1999). The given AR-MA models parameters can be used to reproduce the actual signal PSD of respiratory signals.

Results

The dynamic response compensation in FO_2 and FCO_2 signals allowed us to measure the PSD of respiratory FO_2 and FCO_2 in the range between 0 to 15 Hz. Flow signals were acquired with a PreVent pneumotachometer. The enhanced flow signals could be analyzed in the range between 0 to 50 Hz (the half of sampling frequency) because the cutoff frequency of the employed pneumotachometer plus pressure transducer set is above 50 Hz. The average PSD was calculated separately for each of the four exercise phases. The resulting curves are shown in Figure 1. General mean PSD for all phases combined was also calculated (Figure 2). Parametric ARMA models for these curves are shown in Tables 2 and 3. In all models, m = p = 4.

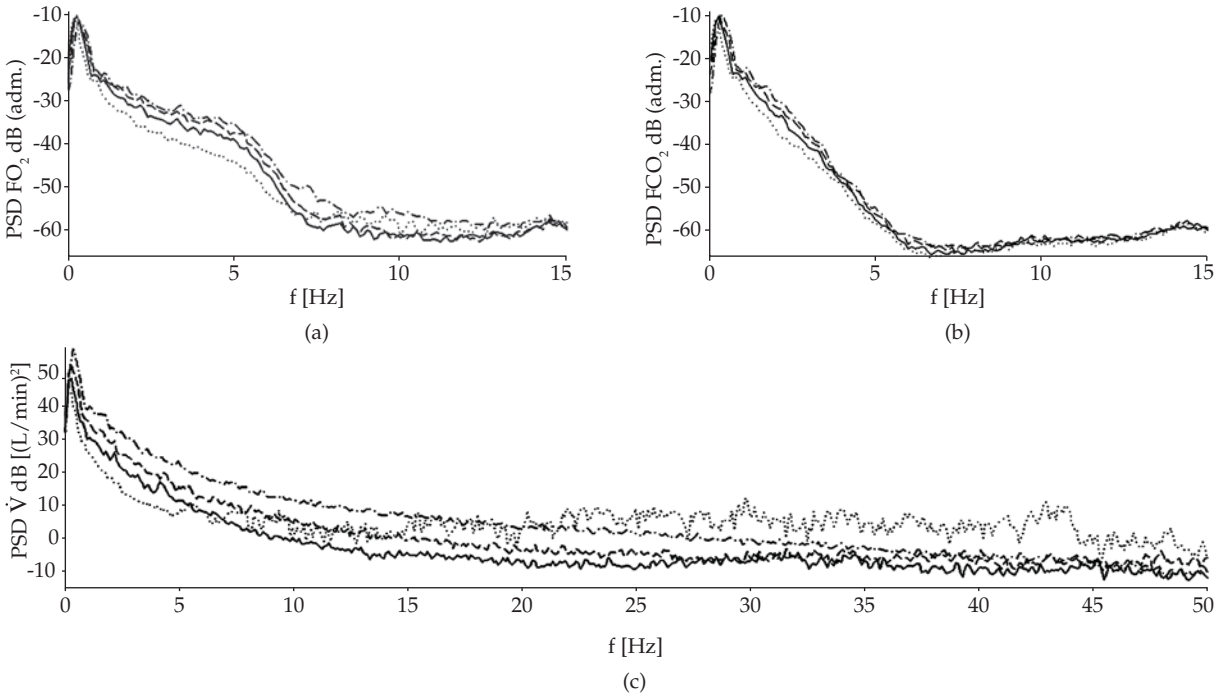

Figure 1. Power spectral densities of respiratory signals (dotted line = phase 1, solid = phase 2, dashed = phase 3, dashdot = phase 4). a) FO_2, b) FCO_2, c) $\dot{V}$.

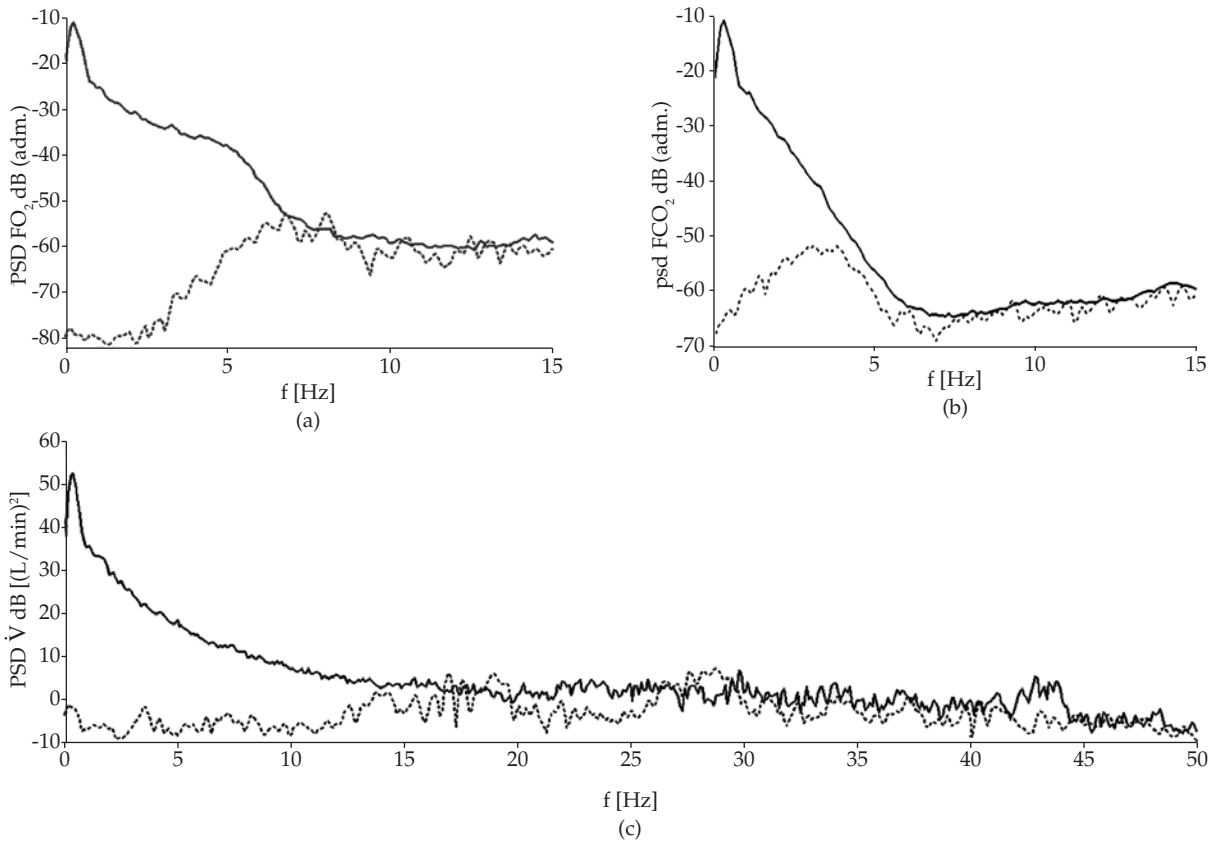

Figure 2. Solid lines: average power spectral densities. a) FO_2, b) FCO_2, c) $\dot{V}$. Dashed lines: respective acquisition background noise.

Table 2. Zeroes and poles of AR-MA models of FO_2 and FCO_2 signals.

First phase			
FO_2 (k = 0.001715)		FCO_2 (k = 0.000939)	
Zeroes	Poles	Zeroes	Poles
0.97888	0.99429 + 0.01514j	0.98820	0.99455 + 0.01358j
0.76910 + 0.38238j	0.99429 – 0.01514j	0.85276 + 0.34852j	0.99455 – 0.01358j
0.76910 – 0.38238j	0.85667 + 0.22609j	0.85276 – 0.34852j	0.87425 + 0.10066j
0.56615	0.85667 – 0.22609j	0.48184	0.87425 – 0.10066j
Second phase			
FO_2 (k = 0.001514)		FCO_2 (k = 0.001025)	
Zeroes	Poles	Zeroes	Poles
0.98255	0.99453 + 0.01797j	0.99092	0.99441 + 0.01609j
0.78252 + 0.44405j	0.99453 – 0.01797j	0.85170 + 0.35027j	0.99441 – 0.01609j
0.78252 – 0.44405j	0.88788 + 0.24834j	0.85170 – 0.35027j	0.90292 + 0.11087j
0.44290	0.88788 – 0.24834j	0.50337	0.90292 – 0.11087j
Third phase			
FO_2 (k = 0.001636)		FCO_2 (k = 0.001053)	
Zeroes	Poles	Zeroes	Poles
0.99132	0.99504 + 0.01821j	0.99455	0.99451 + 0.01740j
0.76273 + 0.46278j	0.99504 – 0.01821j	0.84244 + 0.34590j	0.99451 – 0.01740j
0.76273 – 0.46278j	0.88835 + 0.24777j	0.84244 – 0.34590j	0.91869 + 0.11349j
0.42801	0.88835 – 0.24777j	0.49568	0.91869 – 0.11349j
Fourth phase			
FO_2 (k = 0.001809)		FCO_2 (k = 0.001142)	
Zeroes	Poles	Zeroes	Poles
0.99427	0.99424 + 0.02167j	0.99557	0.99406 + 0.02161j
0.72449 + 0.41627j	0.99424 – 0.02167j	0.84099 + 0.35132j	0.99406 – 0.02161j
0.72449 – 0.41627j	0.89121 + 0.25167j	0.84099 – 0.35132j	0.92565 + 0.11787j
0.39223	0.89121 – 0.25167j	0.52344	0.92565 – 0.11787j
Average between all phases			
FO_2 (k = 0.001700)		FCO_2 (k = 0.001040)	
Zeroes	Poles	Zeroes	Poles
0.98241	0.99361 + 0.01915j	0.99020	0.99333 + 0.01759j
0.75981 + 0.42934j	0.99361 – 0.01915j	0.84858 + 0.34953j	0.99333 – 0.01759j
0.75981 – 0.42934j	0.88647 + 0.25133j	0.84858 – 0.34953j	0.91304 + 0.11140j
0.44021	0.88647 – 0.25133j	0.50500	0.91304 – 0.11140j

Values are non–dimensional.

The background noise level in the flow signal was around the 0 dB level according to Figure 2c. For gas transducers, the background noise level stated around –59 dB in FO_2 signals (Figure 2a) and –62 dB in FCO_2 signals (Figure 2b). We noticed a slight ascending curve in background noise of FCO_2 (Figure 1b). Such background noise is originated from the semiconductor used to detect the infrared light across the gas chamber and the electronic amplifiers embedded in the transducer.

Due to those background noise levels we could observe the spectral components of FO_2 above the background noise level between 0 Hz and 8 Hz approximately, and between 0 Hz and 7 Hz approximately for FCO_2 signals. These thresholds correspond to the inflection points that can be observed near 8 Hz and 7 Hz in Figure 2a and Figure 2b, respectively. Above these frequencies, the observed PSD corresponds to the background noise PSD.

The spectral analysis of $\dot{V}$ could be done for the entire dynamic range between 0 Hz and 50 Hz, due to the good signal to-noise ratio of the transducer in the whole spectral range. Figure 1c shows that the peak power in the $\dot{V}$ spectral density curve increases with the increase of exercise intensity. This occurred because the greater the exercise intensity, the greater the $\dot{V}$ signal amplitude. This can explain that the $\dot{V}$ spectral components in phase 4 stayed above the background noise in the range between 0 Hz and 40 Hz.

Stationary values (less than ±10% in variation) of $\dot{V}O_2$ and $\dot{V}CO_2$ were observed during every 1-minute acquisition session. Although the volunteers per-

Table 3. Zeroes and poles of AR-MA models of $\dot{V}$ signals.

First phase	
$\dot{V}$ (k = 1.931)	
Zeroes	Poles
0.95834	0.99354 + 0.01909j
0.46755 + 0.36175j	0.99354 – 0.01909j
0.46755 – 0.36175j	–0.11306 + 0.40498j
–0.63779	–0.11306 – 0.40498j
Second phase	
$\dot{V}$ (k = 0.718)	
Zeroes	Poles
0.99194	0.99545 + 0.01590j
0.43848 + 0.42252j	0.99545 – 0.01590j
0.43848 – 0.42252j	0.84702
–0.58447	–0.39407
Third phase	
$\dot{V}$ (k = 1.057)	
Zeroes	Poles
0.99580	0.99566 + 0.01834j
0.28720 + 0.28055j	0.99566 – 0.01834j
0.28720 – 0.28055j	0.85267
–0.56653	–0.50937
Fourth phase	
$\dot{V}$ (k = 1.705)	
Zeroes	Poles
0.99785	0.99515 + 0.02281j
0.35062 + 0.09988j	0.99515 – 0.02281j
0.35062 – 0.09988j	0.84833
–0.59152	–0.00256
Average between all phases	
$\dot{V}$ (k = 1.690)	
Zeroes	Poles
0.99020	0.99556 + 0.02159j
0.50102 + 0.38076j	0.99556 – 0.02159j
0.50102 – 0.38076j	0.79464
–0.68345	–0.29090

Values are non-dimensional.

formed the exercise near the respiratory compensation point in Phase 4, we observed that their respiratory signals could reach a stationary behavior after 3 to 4 minutes of performing under this stress condition. A stationary signal is a non-negligible requirement for a good PSD estimation.

Discussion

The main difference in the PSD between exercise phases is located in lower frequencies. As the exercise intensity increases, the peak frequency in all curves increases due to the influence of respiratory rate (peak PSD is at 0.23 Hz in rest and 0.38 Hz in phase 4). The flow peak PSD also increases due to the increasing amplitude of the flow signal by 5 dB at each phase. Figure 1 emphasizes these differences for each signal (FO_2, FCO_2 and $\dot{V}$).

Lemen *et al*. (1982) found the frequency range in $\dot{V}$ between 0 and 5.06 Hz in normal subjects. But, in their measurements, they only considered as significant spectral components the ones with at least 5% of the amplitude of the fundamental. For comparison, if we used their criterion, we would find a frequency range of 2.8 Hz in $\dot{V}$.

The relevance of each phase in the computing of an average PSD of respiratory signals depends on its application. In case of maximal stress tests, measurements are made in the whole range from rest to the maximal capacity of the subject, and the respiratory compensation point is typically exceeded in normal subjects. Therefore, the average PSD prediction for computing the Wiener filters for signal enhancement must consider all four phases analyzed in this paper. In case of a submaximal stress test protocol in which the respiratory compensation point will not be reached, the PSD prediction of the respiratory signals can be computed as an average of Phases 1 to 3, for instance. Another possible procedure could be giving weights for each phase in the average PSD computing, in agreement with the chosen exercise protocol where this average would be employed. The average PSD of respiratory signals shown in Figure 2 and Tables 2 and 3 were computed with equal weight for all four phases.

This research involved healthy adult subjects only. However, special groups of subjects could be interesting for specific applications. These groups could include only children, or chronic obstructive pulmonary disease (COPD) patients, for instance. Specific groups like these can present different flow amplitudes due to reduced tidal volume, different or irregular respiratory rate at rest and under exercise performance, irregular waveform shape of flow and gas concentrations due to irregular respiratory pattern or obstructive diseases, and reduced peak oxygen uptake. The design of optimal filters for specific groups might be necessary to improve the measurements accuracy and is a perspective of continuity to this work.

Conclusions

We acquired human respiratory flow, O_2 concentration and CO_2 concentration signals from 20 healthy subjects in four levels of exercise intensity. Flow signals were filtered with an inverse transducer gain filter for flat gain response in the range between 0 and 50 Hz. O_2 and CO_2 concentration signals were filtered

with Wiener filters for flat gain response between 0 and 15 Hz. Then, we evaluated the PSD curves of those signals and obtained parametric AR-MA models presented in Tables 2 and 3.

Figure 1c shows that $\dot{V}$ signal presented spectral components within a dynamic range of 50 dB in the frequency range between 0 and 10 Hz for averaged subjects in rest, and in the frequency range between 0 and 40 Hz for averaged subjects at 90% RCP. For four-phase averaged PSD (see Figure 2c) flow signal presented spectral components in the range between 0 and 15 Hz.

Figures 1a and 2a show that O_2 concentration spectral components for all phases stayed in the range between 0 and 8 Hz within a dynamic range of 50 dB. Figures 1b and 2b show that CO_2 concentration spectral components for all phases stayed in the range between 0 and 7 Hz within a dynamic range of 50 dB.

Acknowledgements

This work was supported by Fundação de Amparo à Pesquisa do Estado de São Paulo - FAPESP under grants 00/08206-7 and 00/08207-3.

References

AKAIKE, H. Modern development of statistical methods. In: EYKHOFF, P (Ed.). **Trends and progress in system identification**. New York: Pergamon Press, 1981.

ASTRÖM, K. J.; WITTENMARK, B. **Computer-controlled systems - theory and design**. 2 ed. Englewood Cliffs: Prentice Hall, 1990.

ATS/ACCP – American Thoracic Society / American College of Chest Physicians. ATS/ACCP Statement on cardiopulmonary exercise testing. **American Journal of Respiratory and Critical Care Medicine,** v. 167, n. 2, p. 211-277, 2003.

BATES, J. H. T.; PRISK, G. K.; TANNER, T. E.; MCKINNON, A. E. Correcting for the dynamic response of a respiratory mass spectrometer. **Journal of Applied Physiology**, v. 55, n. 3, p. 1015-1022, 1983.

BEAVER, W. L.; WASSERMAN, K.; WHIPP, B. J. A new method for detecting anaerobic threshold by gas exchange. **Journal of Applied Physiology**, v. 60, n. 6, p. 2020-2027, 1986.

FARMERY, A. D.; HAHN, C. E. W. Response-time enhancement of a clinical gas analyzer facilitates measurement of breath-by-breath gas exchange. **Journal of Applied Physiology**, v. 89, n. 2, p. 581-589, 2000.

FERRANNINI, E. The theoretical bases of indirect calorimetry: a review. **Metabolism**, v. 37, n. 3, p. 287-301, 1988.

GARCIA, M. A.; CARDOSO, A. L. R.; SILVA, A. P.; NASCIMENTO, V. H.; MORAES, J. C. T. B. Enhancement of dynamic response of transducers used in ergospirometry with adaptive and Wiener filtering. In: EUROPEAN MEDICAL AND BIOLOGICAL ENGINEERING CONFERENCE EMBEC, 2 , Vienna. Anais… Vienna: IFMBE, 2002, v. 3, p. 1462-1463.

GARCIA, M. A.; MORAES, J. C. T. B. Simple procedure for evaluation of the frequency response of flow transducers used in spirometry and respiratory impedance. **Revista Brasileira de Engenharia Biomédica**, 2008. (in press).

KAILATH, T.; SAYED, A. H.; HASSIBI, B. **Linear estimation.** Upper Saddle River: Prentice Hall, 2000.

LEAR, S. A.; BROZIC, A.; MYERS, J. N.; IGNASZEWSKI, A. Exercise stress testing. An overview of current guidelines. **Sports Medicine**, v. 27, n. 5, p. 285-312, 1999.

LEMEN, R. J.; GERDES, C. B.; WEGMANN, M. J.; PERRIN, K. J. Frequency spectra of flow and volume events for forced vital capacity. **Journal of Applied Physiology**, v. 53, n. 4, p. 977-984, 1982.

LJUNG, L. **System Identification:** Theory for the User. 2 ed. Englewood Cliffs: Prentice Hall, 1999.

MADAMA, V. C. **Pulmonary Function Testing and Cardiopulmonary Stress Testing.** New York: Delmar Publishers, 1993.

MYERS, J.; MADHAVAN, R. Exercise testing with gas exchange analysis. **Cardiology Clinics**, v. 19, n. 3, p. 433-445, 2001.

NOGUCHI, H.; OGUSHI, Y.; YOSHIYA, I.; ITAKURA, N.; YAMABAYASHI, H. Breath-by-breath $\dot{V}O_2$ and $\dot{V}CO_2$ required compensation for transport delay and dynamic response. **Journal of Applied Physiology**, v. 52, n. 1, p. 79-84,1982.

PROAKIS, J.; MANOLAKIS, D. **Digital Signal Processing**. 3 ed. Englewood Cliffs: Prentice-Hall, 1996.

SHYKOFF, B. E.; SWANSON, H. T. Model-free method for mass spectrometer response correction. **Journal of Applied Physiology**, v. 63, n. 5, p. 2148-2153, 1987.

SINGH, V. N. The role of gas analysis with exercise testing. **Primary Care**, v. 28, n. 1, p. 159-179, 2001.

SÖDERSTRÖM, T.; STOICA, P. **System Identification**. Hemel Hempstead: Prentice Hall International, 1989.

WELCH, P. D. The use of fast Fourier transform for the estimation of power spectra: A method based on time averaging over short, modified periodograms. **IEEE Transactions on Audio and Electroacoustics**, v. 15, n. 2, p. 70-73, 1967.

WHITE, R. D.; EVANS, C. H. Performing the exercise test. **Primary Care**, v. 28, n. 1, p. 29-53, 2001.